

# Establishment of Novel Anti-EphB3 Monoclonal Antibodies for Multiple Applications

Guanjie Li, Hiroyuki Suzuki, Mika K. Kaneko, and Yukinari Kato

Ephrin type-B receptor 3 (EphB3) binds to transmembrane ephrin-B ligands to regulate cell migration, adhesion, and proliferation. EphB3 exhibits a gradient expression pattern in the normal intestine, with the highest levels at the crypt base, and plays a crucial role in the maintenance of normal intestinal epithelium. Therefore, anti-EphB3 monoclonal antibodies (mAbs) are required for basic research and diagnosis. In this study, we developed novel antihuman EphB3, Eb<sub>3</sub>Mab-5 (IgG<sub>1</sub>, κ) and Eb<sub>3</sub>Mab-11 (IgG<sub>1</sub>, κ), using the Cell-Based Immunization and Screening (CBIS) method. Eb<sub>3</sub>Mab-5 and Eb<sub>3</sub>Mab-11 reacted with EphB3-overexpressed Chinese hamster ovary-K1 (CHO/EphB3) and endogenous EphB3-positive colorectal cancer LS174T in flow cytometry. The apparent binding affinity of Eb<sub>3</sub>Mab-5 for CHO/EphB3 and LS174T was  $7.6 \times 10^{-9}$  M and  $1.7 \times 10^{-8}$  M, respectively. Eb<sub>3</sub>Mab-11 could detect EphB3 in western blot analysis and immunohistochemistry. Eb<sub>3</sub>Mab-5 and Eb<sub>3</sub>Mab-11, established by the CBIS method, may contribute to the diagnosis and therapy of EphB3-positive tumors.

**Keywords:** EphB3, monoclonal antibody, CBIS method, colorectal cancer, flow cytometry, immunohistochemistry

## Introduction

Receptor tyrosine kinases (RTKs) regulate cell proliferation, differentiation, and motility. About 20 RTK classes have been identified. The Eph receptor family is the largest group of RTKs.<sup>1</sup> The Eph/Ephrin system plays a vital role in normal development<sup>2,3</sup> and diseases such as cancer.<sup>4-6</sup> EphB receptors bind to membrane-bound ephrin B ligands, which regulate tissue homeostasis.<sup>7</sup> In the normal intestine, EphB expression shows a gradient, with the highest levels located at the crypt base.<sup>8</sup> In contrast, the ephrin B ligands display an opposite gradient, with their highest expression at the villus tip.<sup>8</sup> In EphB3-deficient mice, Paneth cells are improperly positioned, being spread along the crypt-villus axis instead of being confined to the crypts.<sup>8</sup>

In the crypt base of the normal intestine, Wnt signaling plays essential roles in maintaining stem cells.<sup>9</sup> Wnt activation causes β-catenin to move to the nucleus and activates β-catenin/TCF target genes like *MYC* and *EPHB3*.<sup>10</sup> Additionally, the ubiquitin ligase Mule promotes the ubiquitination of EphB3 and its degradation via proteasomal and/or lysosomal pathways to limit proliferation and maintain a proper EphB3 gradient.<sup>11</sup>

The constitutive activation of Wnt signaling causes intestinal adenoma development in APC<sup>min</sup> mice.<sup>12</sup> Loss of Mule exacerbates the APC<sup>min</sup> phenotype, suggesting that Mule serves as a tumor suppressor in the intestine through maintenance of proper EphB3 gradient.<sup>11</sup> During colorectal cancer

(CRC) progression, EphB3 shows initial overexpression in early adenoma.<sup>13</sup> EphB3 can suppress CRC migration and invasion by inhibiting AKT.<sup>14</sup> EphB3 exhibits progressive downregulation in advanced tumors, especially at invasive fronts.<sup>15</sup> The downregulation of EphB3 precedes the loss of E-cadherin, indicating its role in initiating the epithelial-mesenchymal transition.<sup>16,17</sup> Clinically, high EphB3 expression is associated with well-differentiated early-stage tumors, whereas its absence in metastatic CRC links to poor differentiation, lymphovascular invasion, and advanced TNM stages.<sup>15</sup> Therefore, the development of anti-EphB3 monoclonal antibodies (mAbs) is crucial for investigating stem cell functions and diagnosing tumors.

We have utilized the Cell-Based Immunization and Screening (CBIS) method to develop mAbs targeting various membrane proteins. The CBIS method involves using cells that overexpress the target antigen as immunogens and screening hybridoma supernatants with flow cytometry. To date, we have successfully generated mAbs against transmembrane proteins, including Eph family<sup>18-20</sup> using the CBIS method. In this study, we generated anti-EphB3 mAbs using the CBIS method and assessed their potential for various applications.

## Materials and Methods

### Antibodies

An anti-human EphB3 mAb (clone 647354, mouse IgG<sub>1</sub>, kappa) was purchased from R&D Systems, Inc. (Minneapolis,

MN, USA). An anti- $\beta$ -actin mAb (clone AC-15) was purchased from Sigma-Aldrich Corp. (St. Louis, MO). Alexa Fluor 488-conjugated anti-mouse IgG was purchased from Cell Signaling Technology, Inc. (Danvers, MA, USA).

#### Preparation of cell lines

Chinese hamster ovary (CHO)-K1, LN229 glioblastoma, P3X63Ag8U.1 (P3U1) myeloma, and human colorectal (LS174T) cell lines were obtained from the American Type Culture Collection (Manassas, VA, USA). The EphB3 complementary DNA (Catalog No.: HGX039581, RIKEN BRC, Ibaraki, JAPAN) was subcloned into a pCAG-Ble vector (FUJIFILM Wako Pure Chemical Corporation, Osaka, Japan). Plasmid transfection into CHO-K1 and LN229 cells was performed using the Neon transfection system (Thermo Fisher Scientific, Inc., Waltham, MA, USA). Stable transfectants (CHO/EphB3 and LN229/EphB3) were then selected with a cell sorter (SH800, Sony Corp., Tokyo, Japan) using an anti-hEphB3 mAb (clone 647354). After sorting, cells were cultured in medium containing 0.5 mg/mL Zeocin (InvivoGen, San Diego, CA, USA). EphB3-knockout LS174T (BINDS-61) was generated using the CRISPR/Cas9 system with EphB3-specific guide RNA (TTCCAGCGCCGGCAGCCGG). These cells and other Eph receptor-expressing CHO-K1 cells (e.g., CHO/EphA2) were cultured as previously described.<sup>18</sup>

#### Production of hybridomas

Animal experiments were approved by the Animal Care and Use Committee of Tohoku University (Permit number: 2022MdA-001) and conducted in accordance with the NIH (National Research Council) Guide for the Care and Use of Laboratory Animals. To develop anti-EphB3 mAbs, two 5-week-old female BALB/cAJcl mice (CLEA Tokyo, Japan) were immunized intraperitoneally with LN229/EphB3 ( $1 \times 10^8$  cells/mouse) starting at 6 weeks of age. Alhydrogel adjuvant 2% (InvivoGen) was added to the immunogen cells during the first immunization. Subsequently, 3 weekly intraperitoneal injections of LN229/EphB3 ( $1 \times 10^8$  cells/mouse) were administered without adjuvant. A final booster injection of  $1 \times 10^8$  LN229/EphB3 cells was given 2 days before harvesting spleen cells from the mice. Cell fusion was performed between harvested splenocytes and P3U1 myeloma cells. The resulting hybridoma supernatants were screened by flow cytometry using CHO/EphB3 and parental CHO-K1 cells. Anti-EphB3 mAbs were purified from the hybridoma supernatants using Ab-Capcher (ProteNova, Kagawa, Japan).

#### Flow cytometric analysis

Cells were harvested using 2.5 g/L-Trypsin/1 mmol/L-EDTA solution with phenol red (Nacalai Tesque, Inc., Kyoto, Japan) and incubated with primary mAbs in phosphate-buffered saline (PBS) containing 0.1% bovine serum albumin for 30 minutes at 4°C. Subsequently, they were stained with Alexa Fluor 488-conjugated anti-mouse (diluted 1:2000) before being analyzed using the SA3800 Cell Analyzer (Sony Corp.).

#### Determination of apparent binding affinity by flow cytometry

CHO/EphB3 and LS174T were suspended in 100  $\mu$ L of serially diluted Eb<sub>3</sub>Mab-5, Eb<sub>3</sub>Mab-11, or 647354, then treated with Alexa Fluor 488-conjugated anti-mouse IgG (dilution 1:200). Fluorescence data were collected using the SA3800 Cell Analyzer, and the apparent binding affinity ( $K_D$ ) was analyzed by fitting the binding isotherms into the built-in one-site binding model in GraphPad PRISM 10 (GraphPad Software, Inc., La Jolla, CA, USA).

#### Western blot analysis

Cell lysates were boiled in sodium dodecyl sulfate sample buffer (Nacalai Tesque, Inc.), then proteins were separated on 5%–20% polyacrylamide gels (FUJIFILM Wako Pure Chemical Corporation) and transferred to polyvinylidene difluoride membranes (Merck KGaA). After blocking with 4% skim milk (Nacalai Tesque, Inc.) in PBS containing 0.05% Tween 20, membranes were incubated with 5  $\mu$ g/mL of Eb<sub>3</sub>Mab-11, 1  $\mu$ g/mL of 647354, or 1  $\mu$ g/mL of anti- $\beta$ -actin mAb (clone AC-15). Then, they were incubated again with horseradish peroxidase-conjugated anti-mouse immunoglobulins (diluted 1:1000; Agilent Technologies, Inc., Santa Clara, CA, USA). Finally, protein bands were detected using ImmunoStar LD (FUJIFILM Wako Pure Chemical Corporation) with a Sayaca-Imager (DRC Co. Ltd., Tokyo, Japan).

#### Immunohistochemistry

Formalin-fixed paraffin-embedded (FFPE) CHO/EphB3 and CHO-K1 blocks were prepared using iPCell (Genostaff Co., Ltd., Tokyo, Japan). The FFPE cell sections were stained with Eb<sub>3</sub>Mab-11 (5  $\mu$ g/mL) and 647354 (5  $\mu$ g/mL) using BenchMark ULTRA PLUS with OptiView DAB IHC Detection Kit or ultraView Universal DAB Detection Kit, respectively (Roche Diagnostics, Indianapolis, IN, USA).

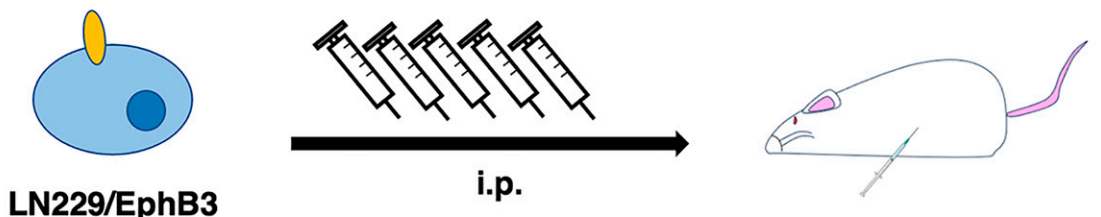
#### Results

##### Establishment of anti-EphB3 mAbs, Eb<sub>3</sub>Mab-5 and Eb<sub>3</sub>Mab-11, using the CBIS method

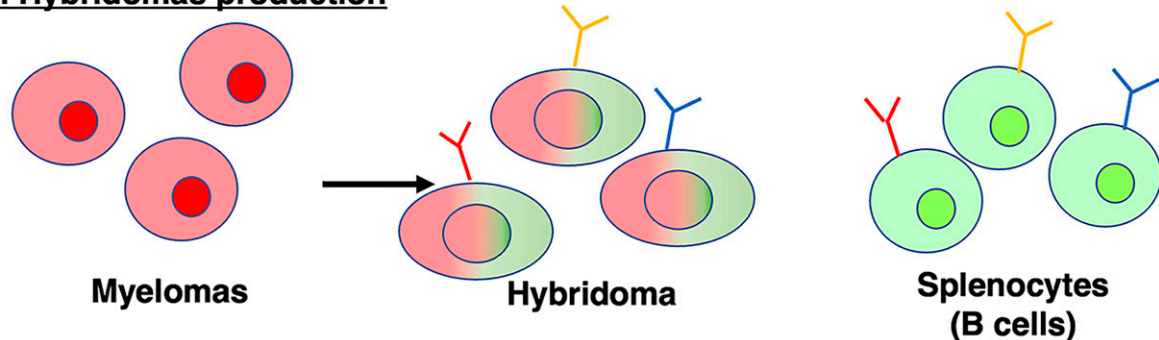
To develop mAbs of anti-EphB3, we employed the CBIS method using EphB3-overexpressed LN229 cells as an antigen. LN229/EphB3 was injected intraperitoneally into female BALB/cAJcl mice (Fig. 1A). The splenocytes were harvested from mice and fused with P3U1 cells (Fig. 1B). After the formation of hybridomas, the supernatants were screened by flow cytometry to identify the CHO/EphB3-reactive supernatants (Fig. 1C). Afterward, we performed limiting dilution of the hybridomas and established clones of anti-EphB3 mAbs (Fig. 1D). We finally established 17 clones and selected Eb<sub>3</sub>Mab-5 (IgG<sub>1</sub>,  $\kappa$ ) and Eb<sub>3</sub>Mab-11 (IgG<sub>1</sub>,  $\kappa$ ) for their applications, including flow cytometry, western blotting, and immunohistochemistry.

After purification of Eb<sub>3</sub>Mab-5 and Eb<sub>3</sub>Mab-11, we conducted flow cytometry to determine the specificity using Eph receptor-overexpressed CHO-K1. As shown in Figure 2, Eb<sub>3</sub>Mab-5 and Eb<sub>3</sub>Mab-11 recognized CHO/EphB3, but not other 13 Eph receptors (EphA1 to A8, A10, B1, B2, B4, and

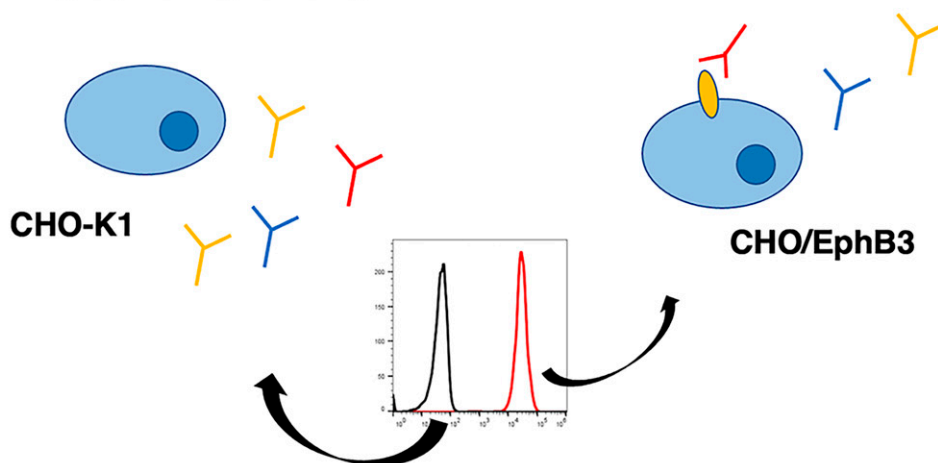
### **A. Immunization of LN229/EphB3**



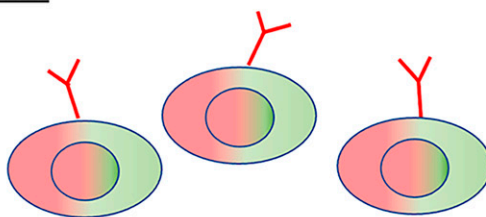
### **B. Hybridomas production**



### **C. Screening by flow cytometry**



### **D. Cloning of Hybridomas**



### **Establishment of anti-EphB3 mAb-producing clones**

**FIG. 1.** Schematic representation of anti-EphB3 mAb development by CBIS method. (A) LN229/EphB3 cells were injected into two female BALB/cAJcl mice. (B) Splenocytes from immunized mice were fused with mouse myeloma P3U1 cells via polyethylene glycol (PEG)-mediated fusion. (C) Culture supernatants of hybridomas were screened using flow cytometry with CHO-K1 and CHO/EphB3 to select EphB3-specific mAb-producing hybridomas. (D) The hybridomas were cloned by limiting dilution. Finally, clones Eb<sub>3</sub>Mab-5 and Eb<sub>3</sub>Mab-11 were established and analyzed.

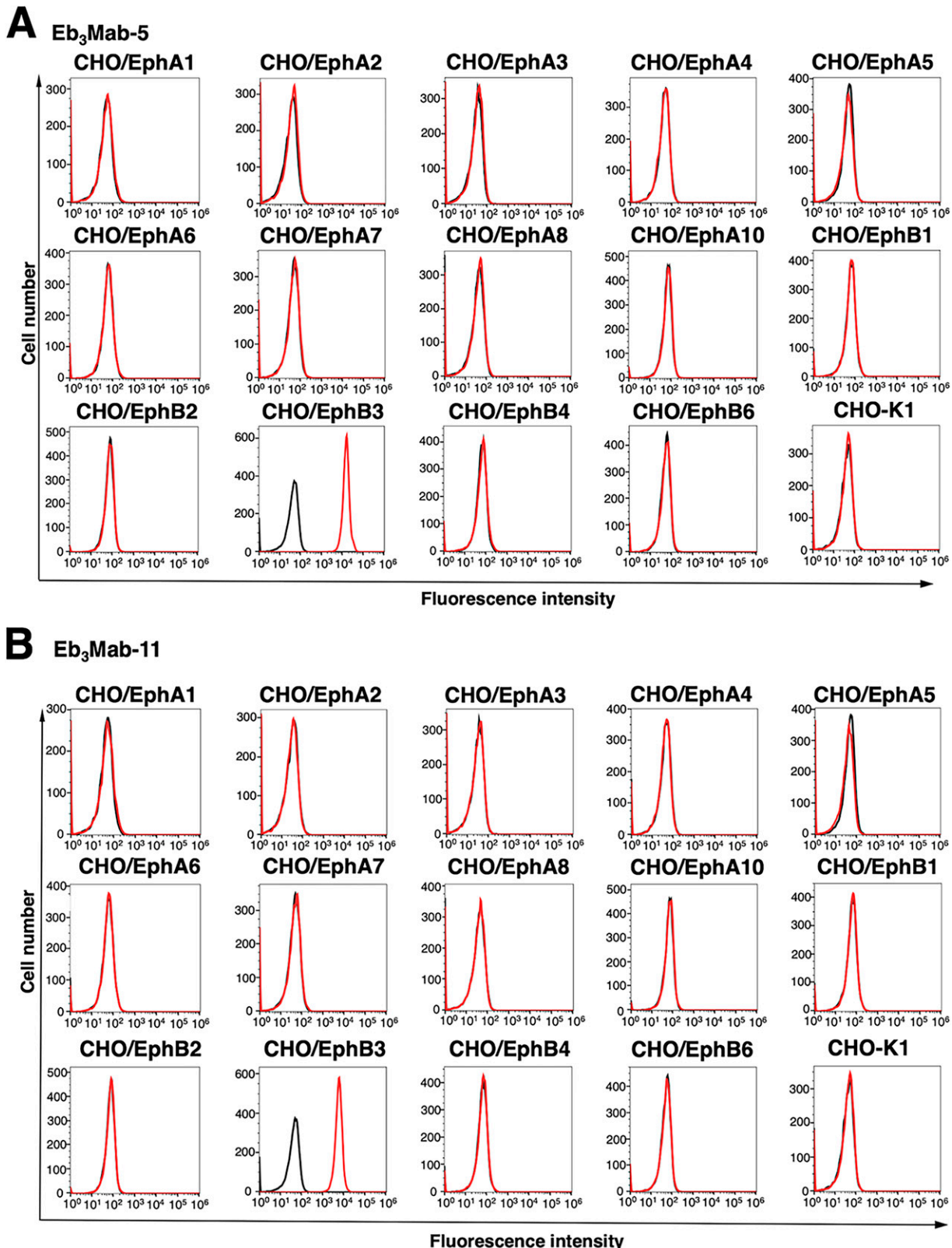


**FIG. 2.** Cross-reactivity of  $\text{Eb}_3\text{Mab-5}$  and  $\text{Eb}_3\text{Mab-11}$  against Eph receptor family. The Eph receptors overexpressed CHO-K1 cell lines were incubated with 10  $\mu\text{g}/\text{mL}$   $\text{Eb}_3\text{Mab-5}$  (Fig. 2A, red line), or  $\text{Eb}_3\text{Mab-11}$  (Fig. 2B, red line), followed by detection with Alexa Fluor 488-conjugated anti-mouse IgG. Fluorescence intensity was detected using the SA3800 Cell Analyzer. The black line represents the negative control (no primary antibody treatment).

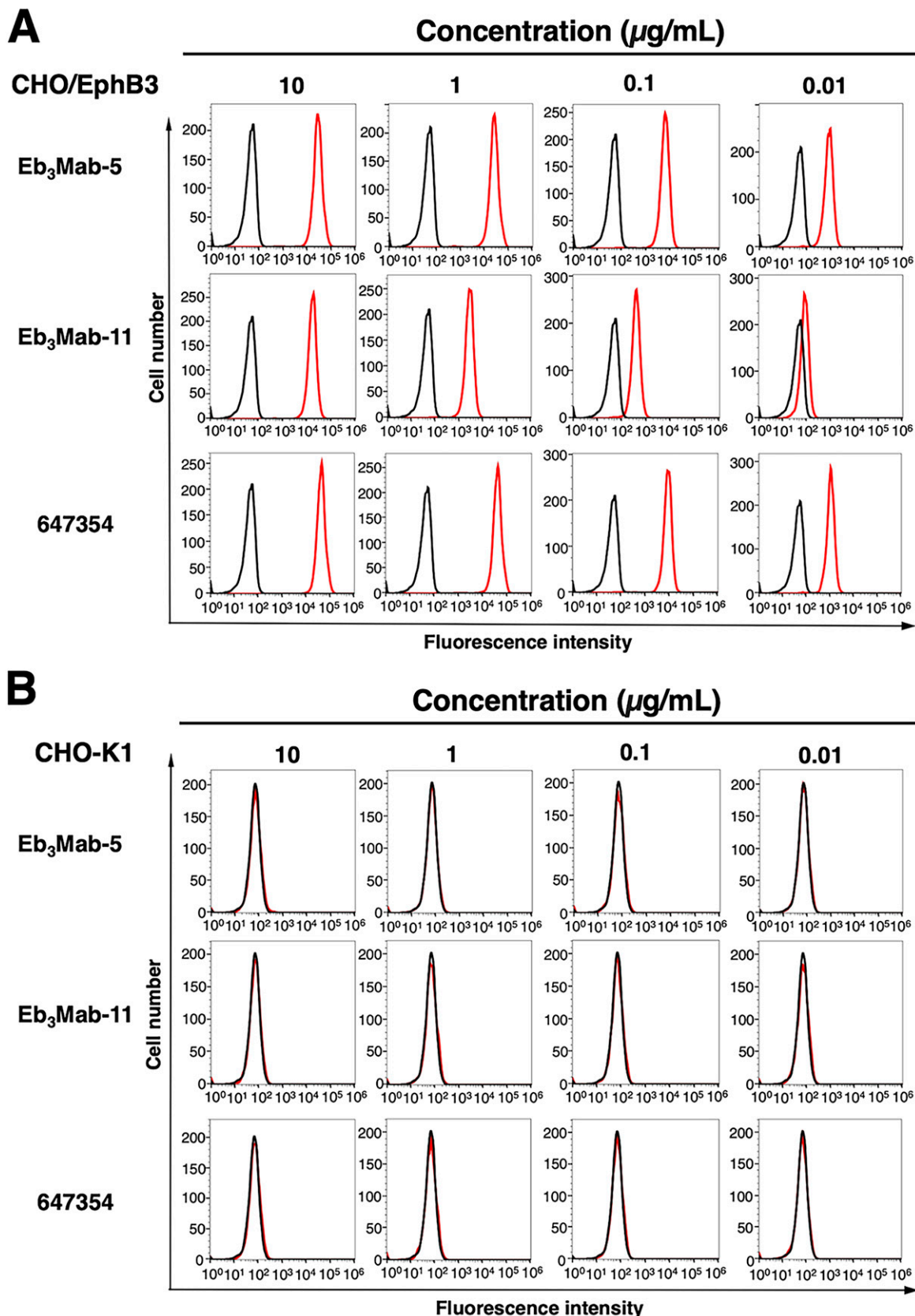


**FIG. 3.** Flow cytometric analysis using anti-EphB3 mAbs. CHO/EphB3 (A) and CHO-K1 (B) cells were incubated with serial concentrations (0.01–10  $\mu\text{g/mL}$ ) of Eb<sub>3</sub>Mab-5, Eb<sub>3</sub>Mab-11, or 647354 (red line), followed by detection with Alexa Fluor 488-conjugated anti-mouse IgG. Fluorescence intensity was measured using the SA3800 Cell Analyzer. The black line represents the negative control (no primary antibody).

B6) (Fig. 2). These results indicated that Eb<sub>3</sub>Mab-5 and Eb<sub>3</sub>Mab-11 can specifically detect EphB3 in flow cytometry.

#### Validation of anti-EphB3 mAb reactivity using flow cytometry

Flow cytometric analysis was performed using Eb<sub>3</sub>Mab-5, Eb<sub>3</sub>Mab-11, and a commercially available anti-EphB3 mAb (clone 647354) on CHO-K1, CHO/EphB3, LS174T, and EphB3-knockout LS174T (BINDS-61) cells. Results showed that Eb<sub>3</sub>Mab-5, Eb<sub>3</sub>Mab-11, and 647354 recognized CHO/EphB3 in a dose-dependent manner (Fig. 3A), but not parental CHO-K1 cells (Fig. 3B). Eb<sub>3</sub>Mab-5, Eb<sub>3</sub>Mab-11, and 647354 also recognized LS174T cells in a dose-dependent manner (Fig. 4A) but not BINDS-61 cells (Fig. 4B). Eb<sub>3</sub>Mab-11 exhibited lower reactivity compared to Eb<sub>3</sub>Mab-5 and 647354. These results indicate that Eb<sub>3</sub>Mab-5 and Eb<sub>3</sub>Mab-11 can detect both endogenous and exogenous EphB3 in flow cytometry.

#### Assessment of binding affinity using anti-EphB3 mAb

The binding affinity of anti-EphB3 mAbs was assessed with CHO/EphB3 and LS174T cells using flow cytometry. The results showed that the apparent binding affinity ( $K_D$ ) of Eb<sub>3</sub>Mab-5 for CHO/EphB3 and LS174T were  $7.6 \times 10^{-9}$  M,  $1.7 \times 10^{-8}$  M, respectively (Fig. 5A). In contrast, the  $K_D$  values of 647354 for CHO/EphB3 and LS174T were  $3.2 \times 10^{-8}$  M and  $2.3 \times 10^{-8}$  M, respectively (Fig. 5B). These results indicate that Eb<sub>3</sub>Mab-5 possesses a higher binding affinity for EphB3-positive cells compared to 647354. In contrast, the binding curves of Eb<sub>3</sub>Mab-11 did not reach a plateau, suggesting lower affinities for those cells (supplementary Fig. S1).

#### Western blot analysis using anti-EphB3 mAbs

Western blot analysis was performed to assess the availability of Eb<sub>3</sub>Mab-11, as preliminary analysis using supernatant from Eb<sub>3</sub>Mabs revealed that only Eb<sub>3</sub>Mab-11 was suitable for western blot analysis. Eb<sub>3</sub>Mab-11 and 647354 detected the  $\sim 100$  kDa band of EphB3 in lysates from CHO/EphB3 (Fig. 6), whereas this band was not present in lysates from CHO-K1. We next performed the detection of endogenous EphB3. A faint 100 kDa band was detected in LS174T, but not BINDS-61 (supplementary Fig. S2). The results indicate that Eb<sub>3</sub>Mab-11 can detect EphB3 in western blot analysis.

#### IHC using anti-EphB3 mAbs

Eb<sub>3</sub>Mab-11 was assessed for immunohistochemistry (IHC) by staining FFPE CHO-K1 and CHO/EphB3 sections. Both Eb<sub>3</sub>Mab-11 (Fig. 7A) and 647354 (Fig. 7B) demonstrated membranous staining in CHO/EphB3 but not in CHO-K1, confirming their availability for IHC to identify EphB3-positive cells in FFPE cell blocks.

## Discussion

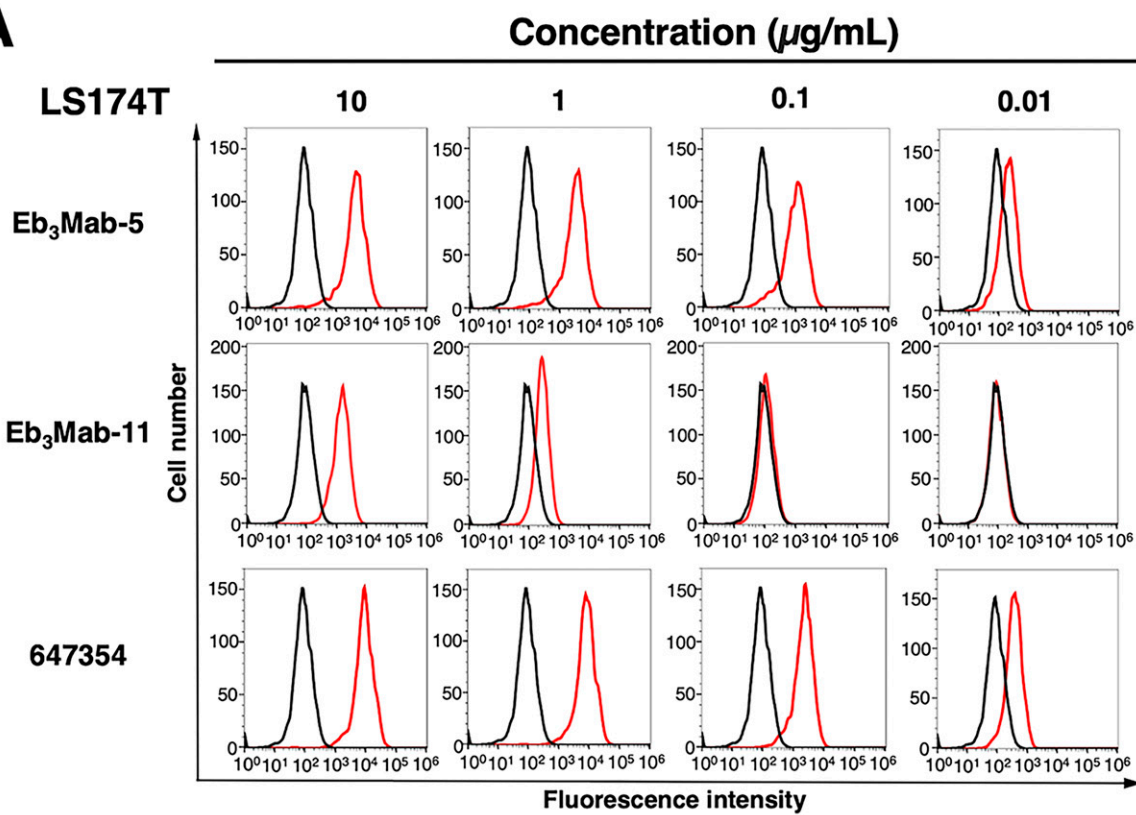
In this study, we developed antihuman EphB3 mAbs, Eb<sub>3</sub>Mab-5 and Eb<sub>3</sub>Mab-11, using the CBIS method (Fig. 1). We demonstrated that both anti-EphB3 mAbs specifically recognize EphB3 in CHO/EphB3 and LS174T cells but not in CHO-K1 or BINDS-61 cells in flow cytometry (Fig. 3 and Fig. 4). Additionally, they do not recognize other Eph-receptor-overexpressed CHO-K1 cells (Fig. 2). Eb<sub>3</sub>Mab-5 has a higher binding affinity for CHO/EphB3 and LS174T (Fig. 5) compared to Eb<sub>3</sub>Mab-11. Conversely, Eb<sub>3</sub>Mab-11 is a versatile mAb for detecting EphB3 in not only flow cytometry, but also western blot (Fig. 6) and IHC (Fig. 7). Since we demonstrated IHC results using FFPE CHO/EphB3 sections, further studies are needed to stain FFPE human colon or colorectal carcinoma tissues. Among 17 clones of Eb<sub>3</sub>Mabs, Eb<sub>3</sub>Mab-11 is the only mAb suitable for multiple applications, and Eb<sub>3</sub>Mab-5 showed the highest reactivity to CHO/EphB3 in flow cytometry. The information of Eb<sub>3</sub>Mabs has been updated on our website “Antibody bank ([http://www.med-tohoku-antibody.com/topics/001\\_paper\\_antibody\\_PDIS.htm](http://www.med-tohoku-antibody.com/topics/001_paper_antibody_PDIS.htm)).

We investigated EphB3 expression in several CRC cell lines using 647354 and found that LS174T exhibited the highest level of EphB3 (Fig. 5). Since we previously confirmed that LS174T can make a tumor xenograft in nude mice,<sup>21</sup> the antitumor efficacy of Eb<sub>3</sub>Mab-5 and Eb<sub>3</sub>Mab-11 could be evaluated in the model. To evaluate the antitumor efficacy of the Eb<sub>3</sub>Mabs, cloning of cDNA and production of class-converted recombinant mAbs are required. We have previously generated mouse IgG<sub>2a</sub>-type, human IgG<sub>1</sub>-type, and humanized recombinant mAbs to confer the antibody-dependent cellular cytotoxicity and complement-dependent cytotoxicity.<sup>21</sup> Using these mAbs, antitumor activities were evaluated using mouse xenograft models.<sup>21,22</sup> We have initiated cloning of the cDNA of Eb<sub>3</sub>Mab-5 and Eb<sub>3</sub>Mab-11 and will evaluate their antitumor efficacy using class-switched (mouse IgG<sub>2a</sub> or human IgG<sub>1</sub>) mAbs.

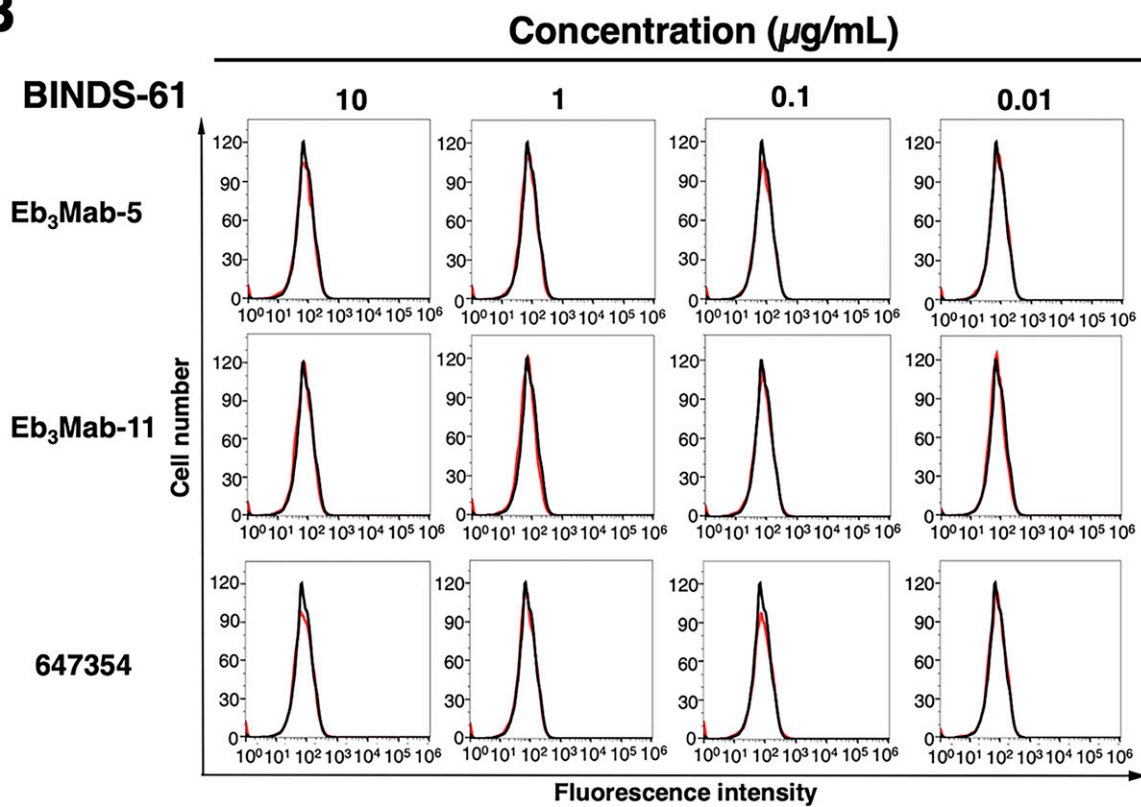
A major challenge in CRC treatment is disease relapse caused by drug resistance.<sup>23</sup> In most CRC cases, patients eventually become resistant to anticancer agents.<sup>23</sup> Cetuximab has antitumor effects by preventing epidermal growth factor (EGF) from attaching to the extracellular part of EGF receptor (EGFR), which stops ligand-driven EGFR signaling.<sup>24</sup> Cetuximab is linked to fewer side effects and has been demonstrated to extend survival in patients with metastatic CRC.<sup>25</sup> Although cetuximab resistance is also observed clinically, the molecular mechanisms remain incompletely understood. Microarray analysis of cetuximab-resistant cells identified EphB3 as involved in resistance through complex formation with EGFR.<sup>26</sup> The EphB3-EGFR complex mediates STAT3 activation induced by EGF and cetuximab treatment in cetuximab-resistant CRC cells.<sup>26</sup> Combination therapy of cetuximab with an EphB3 tyrosine kinase inhibitor (LDN-211904,<sup>27</sup>) showed a potent antitumor efficacy through

**FIG. 4.** Specificity of anti-EphB3 mAbs (Eb<sub>3</sub>Mab-5 and Eb<sub>3</sub>Mab-11) assessed against LS174T and BINDS-61 by flow cytometry. LS174T (A) and BINDS-61 (B) cells were incubated with serial concentrations (0.01–10  $\mu$ g/mL) of Eb<sub>3</sub>Mab-5, Eb<sub>3</sub>Mab-11 or 647354 (red line), followed by detection with Alexa Fluor 488-conjugated anti-mouse IgG. Fluorescence intensity was measured using the SA3800 Cell Analyzer. The black line represents the negative control (no primary antibody).

**A**



**B**



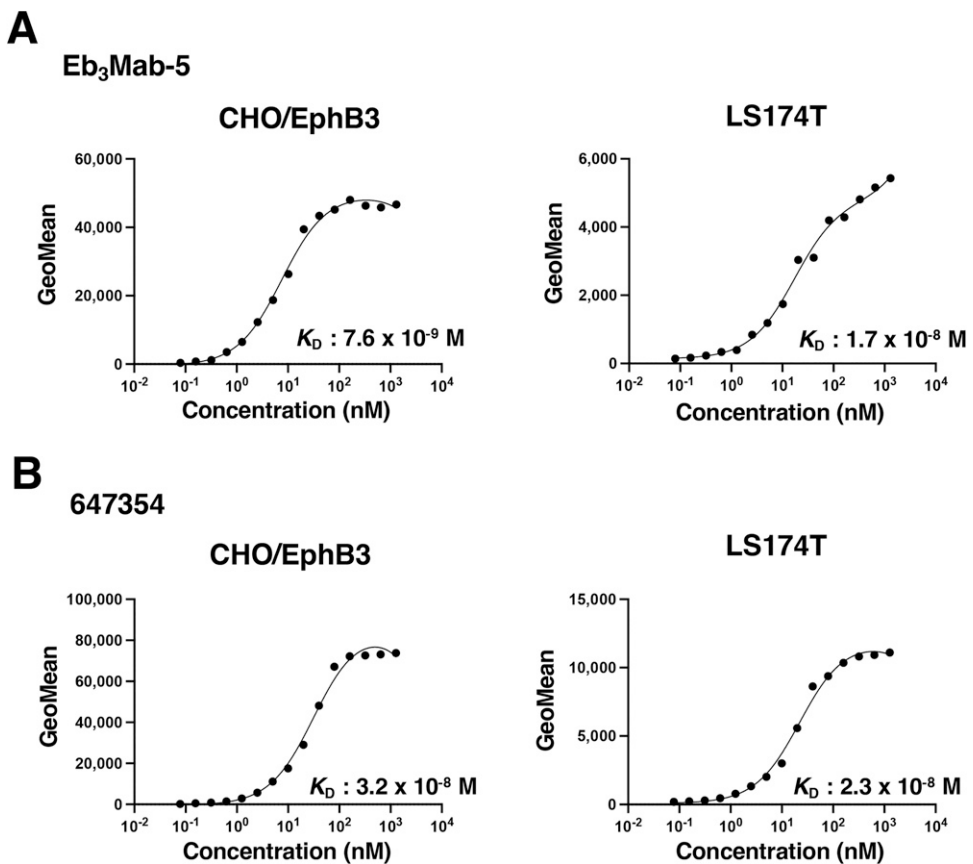


**FIG. 5.** The determination of the apparent binding affinity of anti-EphB3 mAbs. The  $K_D$  values of Eb<sub>3</sub>Mab-5 were evaluated by flow cytometry. CHO/EphB3 and LS174T cells were incubated with serially diluted Eb<sub>3</sub>Mab-5 or 647354 (20  $\mu\text{g}/\text{mL}$ –0.0012  $\mu\text{g}/\text{mL}$ ), followed by detection with Alexa Fluor 488-conjugated anti-mouse IgG, where geometric mean fluorescence values were analyzed using GraphPad PRISM 10 software to determine the  $K_D$  values.

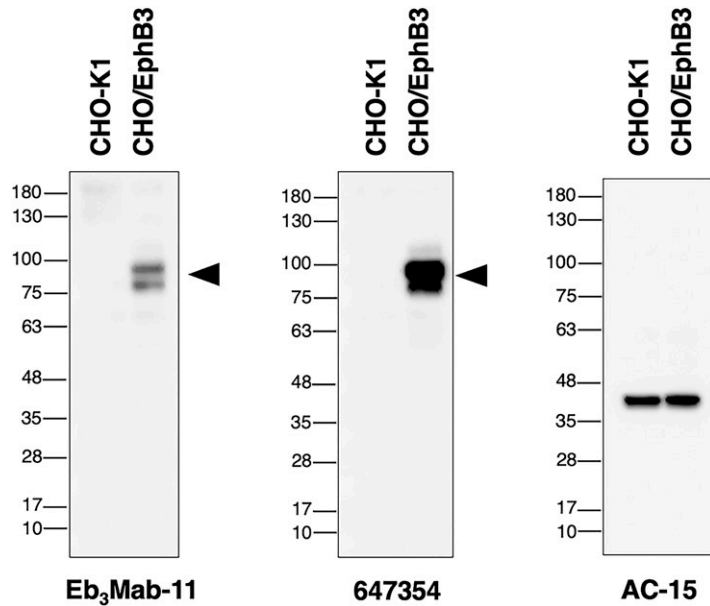


**FIG. 6.** Detection of EphB3 by western blot analysis using anti-EphB3 mAbs. CHO-K1 and CHO/EphB3 cell lysates were electrophoresed, transferred to polyvinylidene fluoride membranes, and incubated with 647354 (1  $\mu\text{g}/\text{mL}$ ), Eb<sub>3</sub>Mab-11 (5  $\mu\text{g}/\text{mL}$ ) and AC-15 (1  $\mu\text{g}/\text{mL}$ ), followed by peroxidase-conjugated anti-mouse immunoglobulins. Black arrow heads indicate the predicted size of EphB3 (~100 kDa).

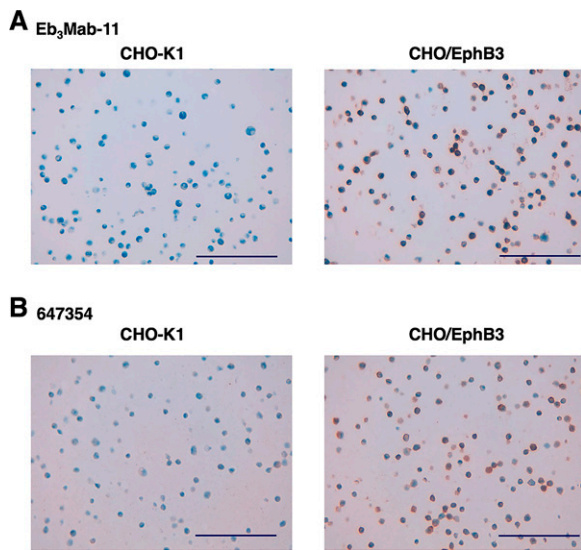


**FIG. 7.** Immunohistochemical analysis using Eb<sub>3</sub>Mab-11 against paraffin-embedded CHO/EphB3 section. The sections of CHO/EphB3 and CHO-K1 were performed using BenchMark ULTRA PLUS. **(A)** The sections were treated with Eb<sub>3</sub>Mab-11 (5 µg/mL) and detected by the Optiview DAB IHC Detection Kit, and **(B)** sections treated with 647354 (5 µg/mL) and detected by the UltraView Universal DAB Detection Kit. Scale bar = 100 µm; magnification, ×400.

inhibition of STAT3-activation in the cetuximab-resistant CRC xenograft.<sup>26</sup> Anti-EphB3 mAbs, which inhibit the EphB3-EGFR complex formation, may overcome cetuximab resistance. Therefore, analyses of the binding epitope and biological activity of Eb<sub>3</sub>Mabs are necessary. Additionally, a class-switched mAb derived from Eb<sub>3</sub>Mabs might enhance therapy for cetuximab-resistant CRC.

#### Authors' Contributions

G.L. performed the experiments. G.L. and H.S. analyzed the data. Y.K. and M.K.K. designed the experiments. G.L., H.S., and Y.K. wrote the article. All authors have read and agreed to the published version of the article.

#### Data Availability Statement

The data and materials that support the findings of this study are available on request from the corresponding author.

#### Author Disclosure Statement

No competing financial interests exist.

#### Funding Information

This research was supported in part by Japan Agency for Medical Research and Development (AMED) under Grant Numbers: JP25am0521010 (to Y.K.), JP25ama121008 (to Y.K.), JP25ama221153 (to Y.K.), JP25ama221339 (to Y.K.), and JP25bm1123027 (to Y.K.), and by the Japan Society for the Promotion of Science (JSPS) Grants-in-Aid for Scientific Research (KAKENHI) grant nos. 25K18843 (to G.L.) and 25K10553 (to Y.K.).

#### Supplementary Material

Supplementary Figure S1  
Supplementary Figure S2

#### References

- Pasquale EB. Eph receptors and ephrins in cancer progression. *Nat Rev Cancer* 2024;24(1):5–27; doi: 10.1038/s41568-023-00634-x
- Zhu Y, Su SA, Shen J, et al. Recent advances of the Ephrin and Eph family in cardiovascular development and pathologies. *iScience* 2024;27(8):110556; doi: 10.1016/j.isci.2024.110556
- Krasewicz J, Yu WM. Eph and ephrin signaling in the development of the central auditory system. *Dev Dyn* 2023; 252(1):10–26; doi: 10.1002/dvdy.506
- Scarini JF, Gonçalves MWA, de Lima-Souza RA, et al. Potential role of the Eph/ephrin system in colorectal cancer: Emerging druggable molecular targets. *Front Oncol* 2024; 14:1275330; doi: 10.3389/fonc.2024.1275330
- Arora S, Scott AM, Janes PW. Eph receptors in cancer. *Biomedicines* 2023;11(2):315; doi: 10.3390/biomedicines11020315
- Papadakos SP, Petrogiannopoulos L, Pergaris A, et al. The EPH/Ephrin system in colorectal cancer. *Int J Mol Sci* 2022;23(5):2761; doi: 10.3390/ijms23052761
- Pasquale EB. Eph receptor signaling complexes in the plasma membrane. *Trends Biochem Sci* 2024;49(12):1079–1096; doi: 10.1016/j.tibs.2024.10.002
- Batlle E, Henderson JT, Beghtel H, et al. Beta-catenin and TCF mediate cell positioning in the intestinal epithelium by controlling the expression of EphB/ephrinB. *Cell* 2002; 111(2):251–263; doi: 10.1016/s0092-8674(02)01015-2
- Beumer J, Clevers H. Cell fate specification and differentiation in the adult mammalian intestine. *Nat Rev Mol Cell Biol* 2021;22(1):39–53; doi: 10.1038/s41580-020-0278-0
- Clevers H. Wnt/beta-catenin signaling in development and disease. *Cell* 2006;127(3):469–480; doi: 10.1016/j.cell.2006.10.018
- Dominguez-Brauer C, Hao Z, Elia AJ, et al. Mule regulates the intestinal stem cell niche via the Wnt pathway and targets EphB3 for proteasomal and lysosomal degradation. *Cell Stem Cell* 2016;19(2):205–216; doi: 10.1016/j.stem.2016.04.002
- Su LK, Kinzler KW, Vogelstein B, et al. Multiple intestinal neoplasia caused by a mutation in the murine homolog of the APC gene. *Science* 1992;256(5057):668–670; doi: 10.1126/science.1350108
- Clevers H, Batlle E. EphB/EphrinB receptors and Wnt signaling in colorectal cancer. *Cancer Res* 2006;66(1):2–5; doi: 10.1158/0008-5472.CAN-05-3849
- Chandrasekera P, Perfetto M, Lu C, et al. Metalloprotease ADAM9 cleaves ephrin-B ligands and differentially regulates Wnt and mTOR signaling downstream of Akt kinase in colorectal cancer cells. *J Biol Chem* 2022;298(8):102225; doi: 10.1016/j.jbc.2022.102225
- Jang BG, Kim HS, Bae JM, et al. Expression profile and prognostic significance of EPHB3 in colorectal cancer. *Bioolecules* 2020;10(4):602; doi: 10.3390/biom10040602
- Mohamet L, Hawkins K, Ward CM. Loss of function of e-cadherin in embryonic stem cells and the relevance to models of tumorigenesis. *J Oncol* 2011;2011:352616; doi: 10.1155/2011/352616
- Theys J, Jutten B, Habets R, et al. E-Cadherin loss associated with EMT promotes radioresistance in human tumor

cells. *Radiother Oncol* 2011;99(3):392–397; doi: 10.1016/j.radonc.2011.05.044

18. Ubukata R, Suzuki H, Hirose M, et al. Establishment of a highly sensitive and specific anti-EphB2 monoclonal antibody (Eb2Mab-12) for flow cytometry. *MI* 2025;2(3):168; doi: 10.36922/mi.5728
19. Satofuka H, Suzuki H, Tanaka T, et al. Development of an anti-human EphA2 monoclonal antibody Ea2Mab-7 for multiple applications. *Biochem Biophys Rep* 2025;42:101998; doi: 10.1016/j.bbrep.2025.101998
20. Satofuka H, Suzuki H, Hirose M, et al. Development of a specific anti-human EphA3 monoclonal antibody, Ea3Mab-20, for flow cytometry. *Biochem Biophys Rep* 2025;43:102130; doi: 10.1016/j.bbrep.2025.102130
21. Ubukata R, Ohishi T, Kaneko MK, et al. EphB2-Targeting monoclonal antibodies exerted antitumor activities in triple-negative breast cancer and lung mesothelioma xenograft models. *Int J Mol Sci* 2025;26(17):8302; doi: 10.3390/ijms26178302
22. Tanaka T, Ohishi T, Asano T, et al. An anti-TROP2 monoclonal antibody TrMab-6 exerts antitumor activity in breast cancer mouse xenograft models. *Oncol Rep* 2021;46(1):132; doi: 10.3892/or.2021.8083
23. Molavand M, Majidinia M, Yousefi B. Critical contribution of various signaling pathways in the development of drug resistance in colorectal cancer: An update. *IUBMB Life* 2025;77(11):e70074; doi: 10.1002/iub.70074
24. Önder AH, Çatlı MM. Colorectal cancer treatment commentary review. *Eur J Cancer* 2025;230:115809; doi: 10.1016/j.ejca.2025.115809
25. Ohishi T, Kaneko MK, Yoshida Y, et al. Current targeted therapy for metastatic colorectal cancer. *Int J Mol Sci* 2023;24(2):1702; doi: 10.3390/ijms24021702
26. Park SH, Jo MJ, Kim BR, et al. Sonic hedgehog pathway activation is associated with cetuximab resistance and EPHB3 receptor induction in colorectal cancer. *Theranostics* 2019;9(8):2235–2251; doi: 10.7150/thno.30678
27. Qiao L, Choi S, Case A, et al. Structure-activity relationship study of EphB3 receptor tyrosine kinase inhibitors. *Bioorg Med Chem Lett* 2009;19(21):6122–6126; doi: 10.1016/j.bmcl.2009.09.010

Address correspondence to:  
Yukinari Kato

Department of Antibody Drug Development  
Tohoku University Graduate School of Medicine  
2-1, Seiryō-machi  
Aoba-ku, Sendai  
Miyagi 980-8575  
Japan

E-mail: yukinari.kato.e6@tohoku.ac.jp

Received: November 14, 2025

Accepted: November 28, 2025